Journal of Power Sources 260 (2014) 163–168

Contents lists available at ScienceDirect

Journal of Power Sources

journal homepage: www.elsevier.com/locate/jpowsour

Short communication

Recycling of the anode from spent Ni-MH batteries for synthesis of the lanthanide oxysulfide/oxysulfate compounds used in an oxygen storage and release system

P.V.M. Dixini [a], V.G. Celante [b], M.F.F. Lelis [a], M.B.J.G. Freitas [a,*]

[a] Federal University of Espírito Santo, Chemistry Department, Laboratory of Electrochemistry and Electroanalytics, Av. Fernando Ferrari, 514, Vitória, ES 29075-910, Brazil
[b] Federal Institute of Espírito Santo, Campus Aracruz, Av. Morobá, 284, Morobá, Aracruz, ES 29192-733, Brazil

HIGHLIGHTS

- Recycling of rare earth metals from anodes of spent Ni-MH batteries.
- Rare earth oxysulfate/oxysulfide for oxygen storage and release system.
- Synthesis of the $(La{\cdot}Nd)_2O_2S{\cdot}CeO_2$ and $(La{\cdot}Nd)_2O_2SO_4CeO_2$ compounds.
- Thermal stability of rare earth oxysulfate/oxysulfide in different atmospheres.

GRAPHICAL ABSTRACT

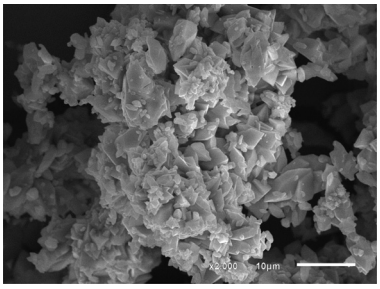

ARTICLE INFO

Article history:
Received 21 January 2014
Received in revised form
1 March 2014
Accepted 5 March 2014
Available online 13 March 2014

Keywords:
Recycling
Nickel metal hydride batteries
Lanthanide oxysulfate
Lanthanide oxysulfide
Oxygen storage system

ABSTRACT

In this work, lanthanide oxysulfide/oxysulfate compounds, denominated as an oxygen storage and release system, have been synthesized from the anode electrodes of spent Ni-MH batteries. The rare earth metals have recovered by means of chemical precipitation as a mixture of $La_2(SO_4)_3$, $Ce_2(SO_4)_3$, and $Nd_2(SO_4)_3$. The synthesis of $(La{\cdot}Nd)O_2S{\cdot}CeO_2$ have been carried out by subjecting a mixture of $La_2(SO_4)_3$, $Ce_2(SO_4)_3$, and $Nd_2(SO_4)_3$ to a heat treatment in a reducing atmosphere up to 1000 °C. The $(La{\cdot}Nd)O_2SO_4{\cdot}CeO_2$ compounds have been obtained after thermal treatment of $(La{\cdot}Nd)O_2S{\cdot}CeO_2$ in a synthetic air atmosphere. The oxysulfide/oxysulfate compounds have been subjected to thermal cycles, respectively, in synthetic air as well as in an N_2–CO atmosphere. The thermogravimetric plot (TG) for $(La{\cdot}Nd)_2O_2S{\cdot}CeO_2$ shows a mass gain of 14.98% w/w in a temperature range of 300–550 °C, which is due to the oxidation of $(La{\cdot}Nd)_2O_2S{\cdot}CeO_2$ to $(La{\cdot}Nd)_2O_2SO_4CeO_2$, where 2 mol of O_2 are added. Likewise, in the $(La{\cdot}Nd)_2O_2SO_4CeO_2$ thermogravimetric plot, a mass loss of 17.16% w/w is observed in the range of 500–750 °C. This loss of mass can be associated with output of 2 mol of O_2 forming again the $(La{\cdot}Nd)_2O_2S{\cdot}CeO_2$. The transformation of the $(La{\cdot}Nd)_2{\cdot}O_2S{\cdot}CeO_2$ to $(La{\cdot}Nd)_2O_2SO_4CeO_2$ causes an increase in the macropores.

1. Introduction

The Ni-MH batteries have as an anode a metal alloy, which in most cases is the type AB_5, where A = La, Ce, Pr, Nd, and B = Ni, Co, Mn and Al. AB_5 alloys have the ability to absorb a large volume of hydrogen as a metal hydride. The cathodes electrodes of these batteries are produced by pressing $Ni(OH)_2$ into the metallic Ni

* Corresponding author. Tel.: +55 27 40097823; fax: +55 27 40092826.
E-mail addresses: marcosbj@hotmail.com, marcosbjg@gmail.com (M.B.J.G. Freitas).

http://dx.doi.org/10.1016/j.jpowsour.2014.03.006
0378-7753/

substrates. Additives such as Co, Zn, and Mn are incorporated into the cathodes to increase the cycle stability and high-rate performance. Ni-MH batteries used in cell phones have lost their market value after the introduction of Li-ion batteries, which have higher energy density. Therefore, a large volume of Ni-MH batteries have become unsuitable for use, having to be discarded as electronic waste. For the rare earth metals, for example, mineral resources are abundant but they extraction and separation requires a high level of technology, which increases the cost of industrial production. In this context, the recycling of spent Ni-MH becomes attractive from economic, ecological, social, and scientific viewpoints [1–4]. The recovery of rare earth metals through a hydrometallurgical method can be performed using techniques such as chemical precipitation, solvent extraction, and metal electrodeposition [5–14]. From the negative electrodes of Ni-MH, compounds such as $(LnO)_2S$ and $(LnO)_2SO_4$ (Ln = La and Nd) can be synthesized, which are denominated as lanthanide oxysulfide and oxysulfate, respectively. They can be applied as an oxygen storage system. Oxygen storage is the ability that certain compounds have to store oxygen into their structure under heating in an oxidizing atmosphere and to release it under heating in a reducing atmosphere. M. Machida et al. [15] studied the thermal and catalytic properties of lanthanide oxysulfides: La, Pr, Nd, and Sm. They concluded that these materials can store and release oxygen at temperatures ranging between 600 and 800 °C, depending on the lanthanide metals used. The highest efficiency was found for $(PrO)_2S$, which was able to absorb oxygen at a temperature of 600 °C. Compounds of type $(LnO)_2S$ and $(LnO)_2SO_4$ (Ln = La, Nd, and Pr) may also be used as catalysts in automotive emission control systems. The catalysts used in automotive systems are currently of the type CeO_2–ZrO_2, capable of absorbing 0.25 mol O_2 per 1 mol of the catalyst. Lanthanide oxysulfide has a higher efficiency and is capable of absorbing up to 2 mol per mol of catalyst, as shown in Eq. (1) [15–20]:

$$Ln_2O_2S + 2O_2 \rightleftarrows Ln_2O_2SO_4 \quad (1)$$

In some cases, the gases released in fuel reforming may contain an amount of sulfur that causes contamination in CeO_2-based catalysts [16]. Systems such as the $(LnO)_2S$ and $(LnO)_2SO_4$ (Ln = La, Nd, and Pr) are able to tolerate significant amounts of sulfur during the catalysis process, making it interesting for applications where there is gaseous sulfur present in the gas mixture.

In the present work, lanthanide oxysulfate/oxysulfide catalysts were synthesized from a mixture of lanthanide sulfates recovered from the anodes of spent Ni-MH batteries. The capacity of the oxygen storage and release of $(La{\cdot}Nd)_2O_2S{\cdot}CeO_2$ and $(La{\cdot}Nd)O_2SO_4.CeO_2$ compounds are analyzed through thermal cycles in synthetic air and an N_2–CO atmosphere, respectively. The structure and composition of the lanthanide oxysulfide/oxysulfate were determined by thermal gravimetric analysis (TGA), X-ray diffraction (XRD), Fourier Transform Infrared Spectroscopy (FT-IR) and scanning electron microscopy (SEM). The recycling efficiency was measured by inductively coupled plasma optical emission spectrometry (ICP OES). The original contribution of this work is the development of a methodology for obtaining lanthanide oxysulfide/oxysulfate catalysts as a good way to recycle the lanthanides present in spent Ni-MH batteries.

2. Experimental

2.1. Characterization of the anodes from spent Ni-MH batteries by XRD and ICP OES

The batteries' composition depends on the type, the manufacturer, and the year manufactured. In this work, Motorola type Ni-MH cellular phone batteries were chosen because a greater amount of these batteries were in household waste. A Ni-MH battery, according to the manufacturer, has a capacity of 1000 mAh and 3.6 V. Spent Ni-MH batteries were physically dismantled and separated into the cathode electrode, consisting of NiOOH/$Ni(OH)_2$, the separators, plastics and packaging, and the anode material placed on the current collector. The anode material was manually separated from the current collector and dried at 50 °C for 3 h. To determine their composition, the anodes materials were characterized by means of XRD and ICP OES. For ICP OES analysis, 1.0 g of the anode material was dissolved in 50.0 mL of HNO_3 7.4 mol L^{-1}.

2.2. Synthesis of the precursor material $Ln_2(SO_4)_3$

L. Li et al. [13] reported the chemical recovery of lanthanides type $Ln_2(SO_4)_3$ with high efficiency. Bertuol et al. [14] established an optimum pH for the recovery of lanthanide sulfates, where process efficiency reaches high values. The most common methods for obtaining lanthanide oxysulfides are: i) from decomposition of commercial $Ln_2(SO_4)_3$ by heating at 900 °C in an N_2 atmosphere for 5 h, followed by heating in an H_2 atmosphere at 800 °C, ii) by a route having the complexation of the lanthanide with an organic sulfonate followed by heating in an H_2 atmosphere at 800 °C [17–20]. In this work, the synthesis of the $Ln_2(SO_4)_3$ (where Ln = La, Ce, and Nd) mixture, was performed weighing 10.0 g of the anode material and then adding to the anode material 500.0 mL of an acid solution made of H_2SO_4 3.0 mol L^{-1} and H_2O_2 30% v v^{-1} in 9:1. The mixture was subjected to constant agitation at a temperature of 80 °C for 2 h to complete solubilization of the anode material. After dissolution, the pH of the solution was 0.2. To obtain the mixture of $Ln_2(SO_4)_3$,solid NaOH was added until the pH reached a value of 1.5, where precipitation of the mixture occurs. The solution was allowed to stand for total decantation of the solid and was filtered under vacuum. The resulting solution after the filtration step was subjected to ICP OES analysis to calculate the recovery efficiency. The filtrate was then dried in an oven at 60 °C for 24 h and characterized by means of XRD and FT-IR techniques.

2.3. Thermal cycling of the $(La{\cdot}Nd)_2O_2S{\cdot}CeO_2$ and $(La{\cdot}Nd)O_2SO_4.CeO_2$ compounds

The $Ln_2(SO_4)_3$ (Ln = La, Ce, and Nd) mixture was heat treated in a gas mixture flow of N_2 and CO (50 mL min^{-1}) with a volume ratio of 2:1, respectively, up to 1000 °C (10 °C min^{-1}), to obtain the $(La{\cdot}Nd)_2O_2S{\cdot}CeO_2$. The residue was collected, and the XRD technique was used for characterization. To evaluate the reduction/reoxidation behavior of the recycled material, $(La{\cdot}Nd)_2O_2S{\cdot}CeO_2$ was submitted to a thermal cycle in the TGA instrument. First, it was oxidized in a synthetic air mixture (50 mL min^{-1}) up to 1000 °C (10 °C min^{-1}) to obtain the oxysulfate phase $(La{\cdot}Nd)O_2SO_4.CeO_2$. After that, it was reduced using in a N_2 and CO mixture (50 mL min^{-1}) up to 1000 °C (10 °C min^{-1}), recovering the oxysulfide $(La{\cdot}Nd)_2O_2S{\cdot}CeO_2$. Both lanthanide oxysulfate and oxysulfide were characterized by means of FT-IR, XRD, and SEM.

2.4. Characterization techniques

All XRD analysis was performed on D8 Advance equipment from Brukker with monochromated Cu Kα radiation. For ICP OES analysis, a Perkin Elmer Optima 7000 DV ICP OES was utilized, using a radial view with a sample flow of 1.5 mL min^{-1} and a power of 1300 W. The FT-IR characterization was made using a Perkin Elmer Spectrum 400 with an ATR (Attenuated Total Reflectance) accessory with a ZnSe crystal. The measurements of TGA/DTGA were performed on a TGA Instruments SDTQ600 using alumina crucibles

and a mass of approximately 20.00 mg. For SEM analysis, a scanning electron microscope, model JEOL 6610LV, was used.

3. Results and discussions

3.1. Characterization of the anode and the leaching solution before and after the rare earth metals recovery

Fig. 1 shows typical X-ray diffraction of the anode from a spent Ni-MH battery. The peaks were compared to the standards of the Joint Committee on Powder Diffraction Standards (JCPDS). The presence of the alloy $LaNi_5$ (JCDPS 12-497), with a hexagonal geometry, can be identified. Metallic Ni (JCDPS 1-1260), with a cubic structure, and Co (JCDPS 1-1278), with a hexagonal structure, are also identified. Cobalt is added to reduce the alloy fragmentation during the absorption/desorption cycles [21]. The concentrations of the constituents in the dissolution solution of the anodes material taken from the Ni-MH batteries are shown in Table 1. It is observed that Ni^{2+} has a higher concentration in the constitution in the dissolution solution of the anodes materials, La^{3+},Ce^{3+},Nd^{3+},and Co^{2+} are also detected. In Table 2 are placed the values of concentrations in the solution for Ni^{2+}, Co^{2+}, La^{3+},Ce^{3+}, and Nd^{3+}, determined by ICP OES, obtained after precipitation and separation of $Ln_2(SO_4)_3$ Ln = La, Ce, Nd. From the data in Tables 1and 2, we can calculate an efficiency of 99.9% for the recovery of lanthanides La, Ce, and Nd. The mass ratio of La, Ce, and Nd present in the recovered material is respectively equal to 6:3:1.

3.2. Characterization of the recycled $Ln_2(SO_4)_3$(Ln = La, Ce, and Nd) by XRD, FT-IR, TG and DTG analyses

The XRD pattern of the rare earth precipitate recovered can be seen in Fig. 2. The peaks were compared to the standards of the Joint Committee on Powder Diffraction Standards (JCPDS). Were identified $La_2(SO_4)_3$ (JCDPS 1-74), $Ce_2(SO_4)_3$ (JCDPS 1-208) and $Nd_2(SO_4)_3$ (JCDPS 23-1265). The infrared spectrum of the recovered material is shown in Fig. 3.Typical sulfate bands are observed in the region of 1000–1150 cm^{-1}. The strong band at 1095 cm^{-1} and the doublet at 1120–1150 cm^{-1} are assigned to the deformation of the S–O bond, while the weaker band at 1003 cm^{-1} is attributed to an oxygen molecule coordinated with the lanthanide sulfate. The peaks for stretching and deformation of the O–H bond are observed in the regions between 3400 and 3650 cm^{-1} and 1616 cm^{-1} respectively, indicating the presence of the adsorbed water molecule [22]. Fig. 4 is the thermogram for the $Ln_2(SO_4)_3$ when subjected to heat treatment in a reducing atmosphere of N_2–CO. A loss of 5.72% w/w of the initial material is observed in the range of 200–320 °C, corresponding to the loss of 2 mol of H_2O, identified by FT-IR analysis. The reaction is represented in the following:

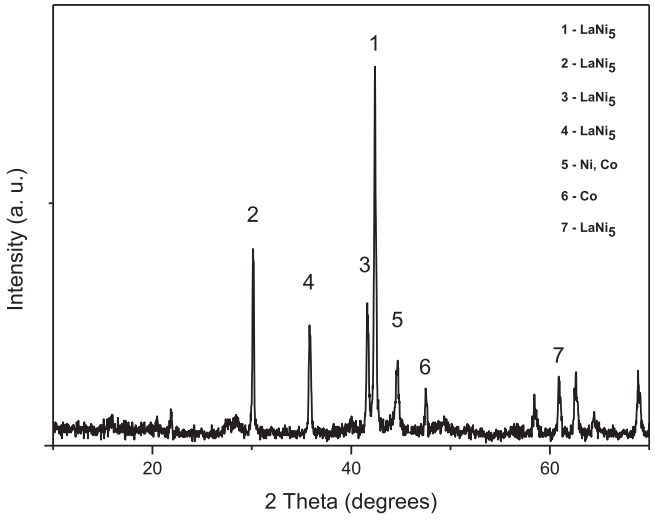

Fig. 1. Typical X-ray diffraction spectrum of the anode electrode from a spent Ni-MH battery.

Table 1
ICP OES analysis results for the solution of the anode material electrode.

Element	Concentration (ppm)
Ni	134.7
Co	14.5
La	47.6
Ce	23.7
Nd	6.7

$$(La\cdot Nd\cdot Ce)_2(SO_4)_3(H_2O)_2 \xrightarrow{279.26\ ^{\circ}C} (La\cdot Nd\cdot Ce)_2(SO_4)_3 + 2H_2O \quad (2)$$

The compound remains thermally stable until 700 °C; in the range of 700 °C–900 °C, a mass loss of 38.78% w/w occurs, forming a stable compound at 900 °C. In the DTGA curve, a peak at 832.98 °C is evidenced; this peak can be associated with the reduction reaction of La and Nd sulfate to oxysulfide phase and the oxidation of carbon monoxide to carbon dioxide [17–19]. The calcination of $Ce_2(SO_4)_3$ under these conditions is not capable of forming Ce_2O_2S. Ce (III) is oxidized to Ce (IV) and the carbon monoxide is oxidized to carbon dioxide [17]. The chemical reactions in the second period of mass loss can be described as:

$$(La\cdot Nd)_2(SO_4)_3 + 2CO \xrightarrow{832.98\ ^{\circ}C} (La\cdot Nd)_2O_2S + 2SO_2 + 2CO_2 + 2O_2 \quad (3)$$

$$Ce_2(SO_4)_3 + 2CO \xrightarrow{832.98\ ^{\circ}C} 2CeO_2 + 3SO_2 + 2CO_2 \quad (4)$$

Overall chemical reaction of the second range of mass loss:

$$(La\cdot Nd\cdot Ce)_2(SO_4)_3 + 4CO \xrightarrow{832.98\ ^{\circ}C} (La\cdot Nd)_2O_2S\cdot 2CeO_2 + 5SO_2 + 4CO_2 + 2O_2 \quad (5)$$

X-ray diffraction of the residue (Fig. 5) was made in addition to the data of TGA and DTG measurements. In the XRD pattern, the presence of $(LaO)_2S$, $(NdO)_2S$ and CeO_2 was detected, which corroborates with the thermal degradation reactions proposed (Eq. (5)). The oxysulfide had a rhombohedral structure (P3m1) similar to that reported by other authors [17] and the cerium (IV) oxide had a cubic structure typical of the CeO_2 used in the CeO_2–ZrO_2 catalysts [17,23]. A comparison between the experimental and theoretical loss of mass is presented in Table 3. Good agreement was

Table 2
ICP OES analysis results for the solution of the anode material electrode after rare earth recuperation.

Element	Concentration after extraction (ppm)
Ni	133.5
Co	13.2
La	0.06
Ce	0.01
Nd	Not detected

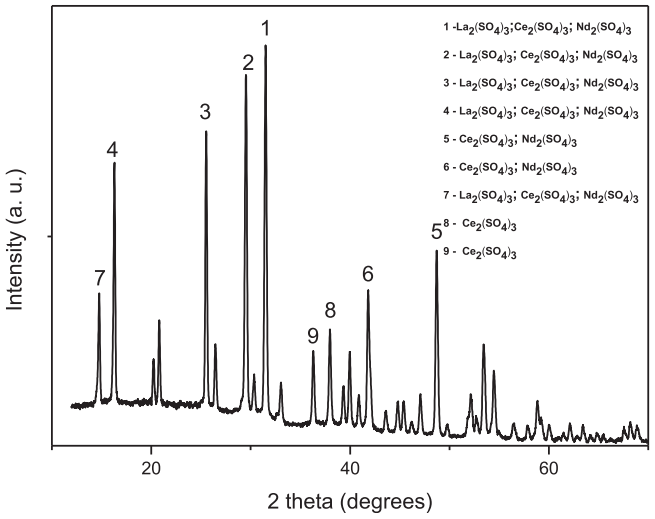

Fig. 2. Typical X-ray diffraction spectrum of the rare earth oxysulfate recovered from the anodes of the spent Ni-MH.

found between the experimental and theoretical results. This confirms t the mechanism for lanthanide oxysulfide/oxysulfate formation.

3.3. Thermal analysis of the$(La{\cdot}Nd)_2O_2S{\cdot}CeO_2and(La{\cdot}Nd)O_2SO_4.CeO_2$ compounds

The $(La{\cdot}Nd)_2O_2S{\cdot}CeO_2$ and $(La{\cdot}Nd)O_2SO_4.CeO_2$ compounds were subjected to thermal cycles in synthetic air and N_2–CO atmospheres, respectively, to verify their capacities as oxygen storage systems. Fig. 6(a) is the thermogram curve for the oxidation of $(LnO)_2S$ and CeO_2. A mass gain of 14.98% w/w can be observed in the temperature range of 300–550 °C. This weight gain is attributed to the oxidation reaction of $(La{\cdot}Nd)_2O_2S{\cdot}CeO_2$ to $(La{\cdot}Nd)O_2SO_4.CeO_2$, where 2 mol of O_2 are added to the oxysulfide molecule. Fig. 6(b) is the thermogram curve for $(La{\cdot}Nd)_2O_2SO_4CeO_2$ in an N_2–CO atmosphere. A mass loss of the 17.16% w/w is observed in the range 500–750 °C, which is associated with the loss of 2 mol of O_2 due to the reduction process. In this case, the $(La{\cdot}Nd)_2O_2S{\cdot}CeO_2$

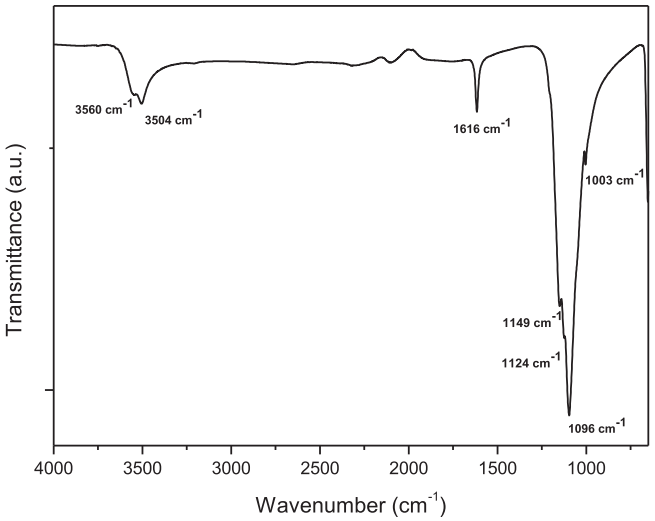

Fig. 3. Infrared spectroscopy spectrum of the rare earth oxysulfate recovered from the anodes of the spent Ni-MH.

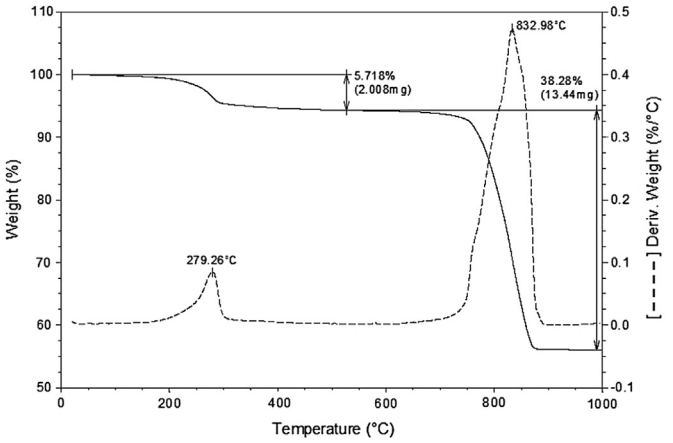

Fig. 4. Thermogravimetric and differential thermogravimetric curves for materials recovered by chemical precipitation: N_2–CO atmosphere, scan rate of 10 °C min^{-1}, alumina crucible.

is regenerated. A regeneration temperature range for the process of oxidation/reduction observed in the recycled material is smaller than that already reported by other authors. The lowest temperature range for these types of catalysts was reported for $(PrO)_2S$ by M. Machida et al. [17], where it is able to oxidize at temperatures above 600 °C.

The materials left after the thermal treatments in oxidizing and reducing atmospheres were characterized by FT-IR and XDR techniques to determine. The FT-IR spectrum of $(La{\cdot}Nd)_2O_2SO_4CeO_2$ is shown in Fig. 7(a). In this Figure, we can observe the presence of peaks relating to the formation of S–O bonds in the region between 990 and 1200 cm^{-1}. The peaks at 1149 cm^{-1} and 1096 cm^{-1} as well as the shoulder at 1124 cm^{-1} are related to the oxygen of the sulfate group that are not coordinated, whereas the weaker peak at 1003 cm^{-1} is relative to the oxygen of the sulfate group coordinated to the metal. In the infrared spectrum of the $(La{\cdot}Nd)_2O_2S{\cdot}CeO_2$, shown in Fig. 7(b), no bands in the infrared region studied were found. This fact is indicative of the oxysulfide formation because the bonds present in this kind of material are of the types S-M and M-O, where M is a metal that does not have activity in this spectra region. XRD analysis was performed in order to identify the products formed after thermal treatment.

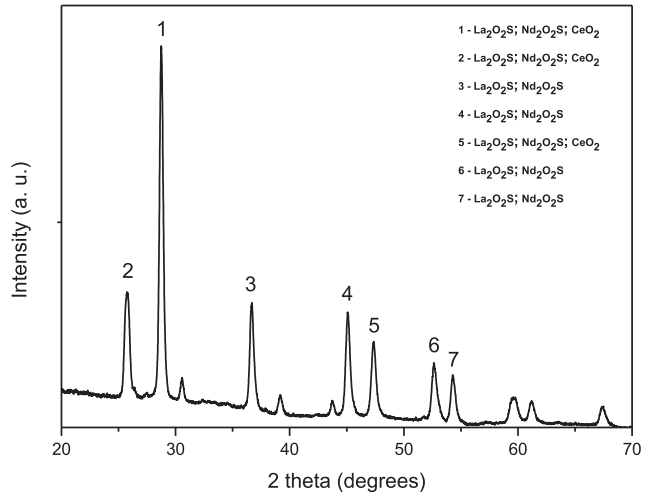

Fig. 5. Typical X-ray diffraction spectrum of the residue of the thermal treatment of the rare earth oxysulfate.

Table 3
Theoretical and experimental values of the mass loss of $Ln_2(SO_4)_3$, where Ln = La and Nd.

Compound	Temperature range (%)	Observed mass loss (%)	Expected mass loss (%)
$La_2(SO_4)_3$	700–886	38.76	39.57
$Nd_2(SO_4)_3$	700–886	38.76	38.88
$Ce_2(SO_4)_3$	700–886	38.76	39.43

In Fig. 8(a) the XRD pattern from the residue, of the heat treatment of $(La{\cdot}Nd)O_2SCeO_2$ in a synthetic air atmosphere, is shown. Peaks of $(LaO)_2SO_4$, $(NdO)_2SO_4$ and CeO_2 are identified. Lanthanum and neodymium oxysulfate both have a monoclinic (C2/c) structure and are in accordance with the material reported in the literature [15–17]. The CeO_2 has the same structure as that obtained in the reduced phase, demonstrating that only lanthanum and neodymium oxysulfides act as store oxygen.

Fig. 8(b) is the diffractogram of the residue of the heat treatment of the $(La{\cdot}Nd)O_2SO_4.CeO_2$ in an N_2–CO atmosphere. The diffraction pattern is similar to that shown in Fig. 5, indicating that $(La{\cdot}Nd)_2O_2S{\cdot}CeO_2$ is formed. The materials have the same crystal structure as those obtained by thermal degradation of the starting material. We notice that there is no evidence of a structural change in CeO_2, which proves that it does not participate in the oxygen storage/release. In agreement with the thermal measurements in addition to the FT-IR and XRD analyses, the chemical reaction is described by Eq. (6):

$$(La{\cdot}Nd)_2O_2S{\cdot}CeO_2 + 2O_2 \rightleftarrows (La{\cdot}Nd)_2O_2SO_4{\cdot}CeO_2 \quad (6)$$

Table 4 shows a comparison between theoretical and experimental values of loss and gain of mass in the thermal cycling of the catalysts. Similar values were found, indicating a good reversibility of recycled material. These results demonstrate that the material obtained by recycling from anodes of spent Ni-MH batteries has a good ability to store and release oxygen.

Fig. 9(a) and (b) show the micrographs of $(La{\cdot}Nd)_2{\cdot}O_2S{\cdot}CeO_2$ and $(La{\cdot}Nd)_2O_2SO_4CeO_2$, respectively. The micrographs of the recycled material show macropores larger than 50 nm. In Fig. 9(a) and (b), we can visualize the formation of agglomerates and large pores between the agglomerates that facilitate the diffusion of gas

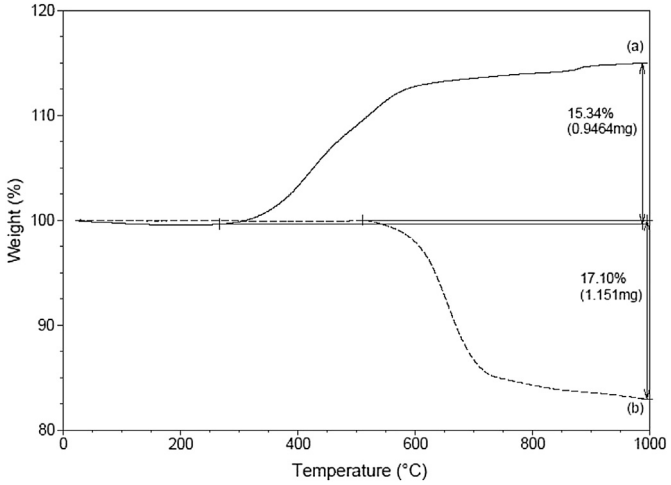

Fig. 6. Thermogravimetric curve for: (a) $(La{\cdot}Nd)_2O_2S{\cdot}CeO_2$, in synthetic air atmosphere and (b) $(La{\cdot}Nd)_2O_2SO_4CeO_2$, in N_2–CO atmosphere.

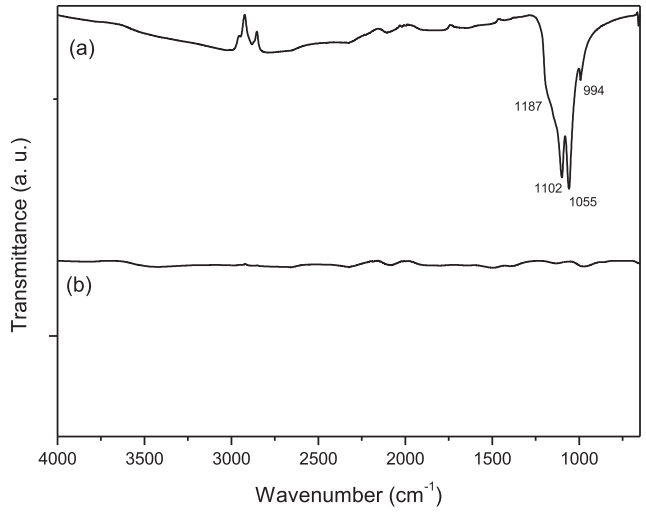

Fig. 7. Infrared spectroscopy spectrum: (a) $(La{\cdot}Nd)_2O_2SO_4CeO_2$and (b) $(La{\cdot}Nd)_2O_2S{\cdot}CeO_2$.

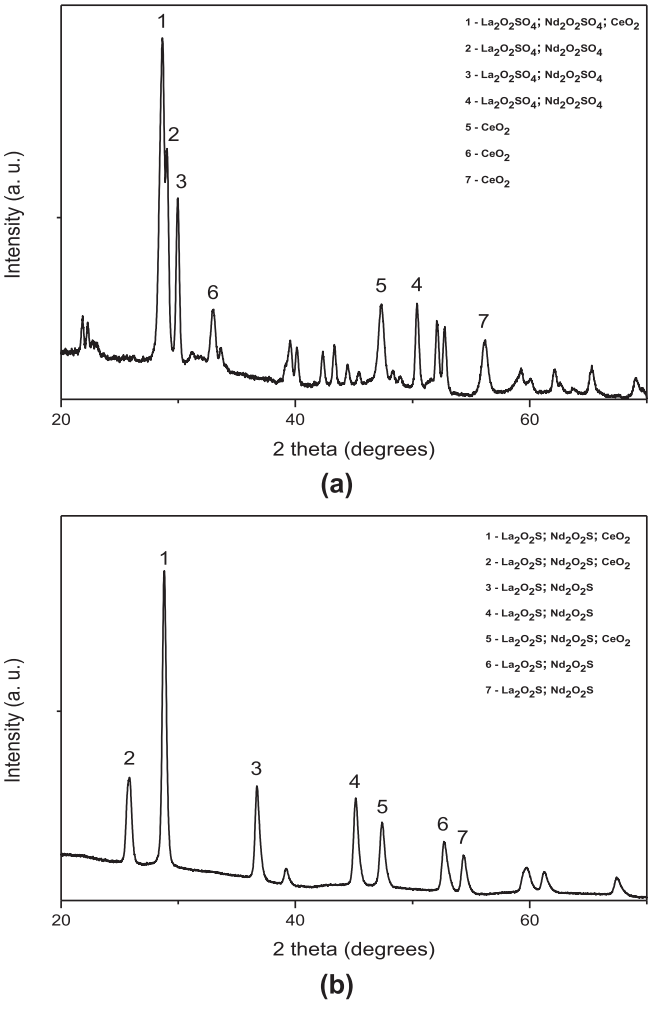

Fig. 8. Typical X-ray diffraction spectrum of the residue of the heat treatment of the: (a) $(La{\cdot}Nd)O_2SCeO_2$ in synthetic air atmosphere and (b) $(La{\cdot}Nd)O_2SO_4.CeO_2$ in N_2–CO atmosphere.

Table 4
Theoretical and experimental values of the mass loss of $(LnO)_2S/(LnO)_2SO_4$, where Ln = La and Nd.

Compounds	Observed mass gain (%)	Expected mass gain (%)	Observed mass loss (%)	Expected mass loss (%)
$(LaO)_2S/(LaO)_2SO_4$	14.98	15.76	17.16	15.76
$(NdO)_2S/(NdO)_2SO_4$	14.98	15.40	17.16	15.40

into the material. The transformation of the $(La{\cdot}Nd)_2{\cdot}O_2S{\cdot}CeO_2$ to $(La{\cdot}Nd)_2O_2SO_4CeO_2$ causes an increase in the macropores in the agglomerates and the formation of a crystalline structure in the format of a micro-plate. A structural transformation from a rhombohedral structure to a monoclynic one occurs when the $(La{\cdot}Nd)_2O_2SO_4CeO_2$ phase is obtained from the $(La{\cdot}Nd)_2{\cdot}O_2S{\cdot}CeO_2$ phase in the thermal oxidation process. The variation of the molar volume provokes the disruption in the agglomerates of the $(La{\cdot}Nd)_2{\cdot}O_2S{\cdot}CeO_2$ phase. This disruption causes the increase of the macroporosity visualized in Fig. 9(b).

4. Conclusion

In this work, the chemical recycling of the anode from spent Ni-MH batteries was studied. The rare earth metals were recovered by means of chemical precipitation as $La_2(SO_4)_3$, $Ce_2(SO_4)_3$, and $Nd_2(SO_4)_3$, and an efficiency of 99.0%, determined by ICP OES, has been reached. The synthesis of $(La{\cdot}Nd)O_2SO_4.CeO_2$(Ce does not form oxysulfide) was carried out by subjecting the mixture of $La_2(SO_4)_3$, $Ce_2(SO_4)_3$, and $Nd_2(SO_4)_3$ to a heat treatment of up to 1000 °C in a reducing atmosphere. The $(La{\cdot}Nd)_2O_2S{\cdot}CeO_2$ and $(La{\cdot}Nd)O_2SO_4.CeO_2$ compounds were subjected to thermal cycles in synthetic air and N_2–CO atmospheres, respectively, to verify their capacities to store and release oxygen. In the TGA plot for $(La{\cdot}Nd)_2O_2S{\cdot}CeO_2$,a mass gain of 14.98% w/w can be observed, in the temperature range of 300–550 °C, attributed to the oxidation of the $(La{\cdot}Nd)_2O_2S{\cdot}CeO_2$ to $(La{\cdot}Nd)_2O_2SO_4CeO_2$, where 2 mol of O_2 molecules are added to the $(La{\cdot}Nd)_2O_2S{\cdot}CeO_2$. In the TGA curve for $(La{\cdot}Nd)_2O_2SO_4CeO_2$,a mass loss of 17.16% w/w is observed in the range of 500–750 °C. This mass loss is associated with the release of 2 O_2mol, forming again the $(La{\cdot}Nd)_2O_2S{\cdot}CeO_2$. The transformation of the $(La{\cdot}Nd)_2{\cdot}O_2S{\cdot}CeO_2$ to $(La{\cdot}Nd)_2O_2SO_4CeO_2$ causes an increase in the macropores within the agglomerates and the formation of a crystalline structure in a micro-plate format. We can conclude that this methodology proved feasible for obtaining this kind of catalyst, producing stable materials. It is a similar activity to those obtained through pure reagents and also an efficient way to recycle the lanthanides present in spent Ni-MH batteries.

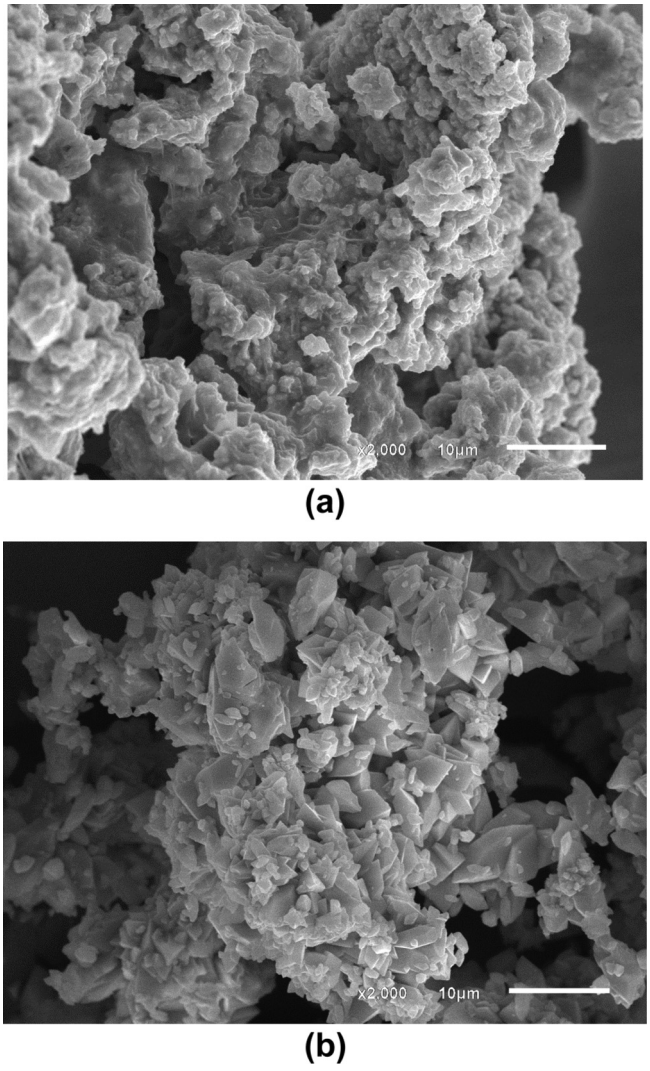

Fig. 9. Micrographs of the materials recovered: (a) $(LnO)_2S{\cdot}CeO_2$ and (b) $(LnO)_2SO_4.CeO_2$.

Acknowledgments

The authors would like to thank the UFES, Laboratório Ultraestrutura Celular CCS/UFES, FAPES, Coordenação de Aperfeiçoamento de Pessoal de Nível Superior and NCQP for their financial support.

References

[1] M.A.R. Rocio, M.M. da Silva, P.S.L. de Carvalho, J.G.R. Cardoso, BNDES Setorial 35 (2012) 369–420.
[2] K. Scott, Nickel-Metal Hydride Batteries, Encyclopedia of Electrochemical Power Sources, Elsevier, New York, 2009, pp. 198–208.
[3] D.A. Bertuol, A.M. Bernardes, J.A.S. Tenorio, J. Power Sources 193 (2009) 914–923.
[4] K. Provazi, B.A. Campos, D.C.R. Espinosa, J.A.S. Tenorio, Waste Manag. 31 (2011) 59–64.
[5] V.E.O. Santos, V.G. Celante, M.F.F. Lelis, M.B.J.G. Freitas, J. Power Sources 218 (2012) 435–444.
[6] M.A. Rabah, F.E. Farghaly, M.A. Abd-El Motaleb, Waste Manag. 28 (2008) 1159–1167.
[7] M.B.J.G. Freitas, J. Power Sources 93 (2001) 163–173.
[8] M.B.J.G. Freitas, D.M. Anjos, P.G. Manoel, A. Rozario, R.K.S.E. Silva, J. Power Sources 162 (2007) 916–921.
[9] D.C.R. Espinosa, A.M. Bernardes, J.A.S. Tenório, J. Power Sources 135 (2004) 311–319.
[10] T. Muller, B. Friedrich, J. Power Sources 158 (2006) 1498–1509.
[11] L.E.O.C. Rodrigues, M.B. Mansur, J. Power Sources 195 (2010) 3735–3741.
[12] N. Tzanetakis, K. Scott, J. Chem. Technol. Biotechnol. 79 (2004) 927–934.
[13] L. Li, S. Xu, Z. Ju, F. Wu, Hydrometallurgy 100 (2009) 41–46.
[14] D.A. Bertuol, F.D.R. Amado, H. Veit, J.Z. Ferreira, A.M. Bernardes, Chem. Eng. Technol. 35 (2012) 2084–2092.
[15] M. Machida, K. Kawamura, K. Ito, K. Ikeue, Chem. Mater. 17 (2005) 1487–1492.
[16] I. Valsamakis, M. Flytzani-Stephanopoulos, Appl. Catal. B Environ. 106 (2011) 255–263.
[17] W. Deng, J. Jesus, H. Saltsburg, M. Flytzani-Stephanopoulos, Appl. Catal. A Gen. 291 (2005) 126–135.
[18] M. Machida, T. Kawano, M. Eto, D. Zhang, K. Ikeue, Chem. Mater. 19 (2007) 954–960.
[19] K. Ikeue, T. Kawano, M. Eto, D. Zhang, M. Machida, J. Alloy Compd. 451 (2008) 338–340.
[20] D. Zhang, F. Yoshioka, K. Ikeue, M. Machida, Chem. Mater. 20 (2008) 6697–6703.
[21] A.S. Pratt, D.B. Willey, I.R. Harris, Platin. Met. Rev. 43 (1999) 50–58.
[22] A.V. Santos, A.S.M. Simões, A.G. Souza, J.R. Matos, Quim. Nova 24 (2001) 320–323.
[23] J.A. Poston Jr., R.V. Siriwardane, E.P. Fisher, A.L. Miltz, Appl. Surf. Sci. 214 (2003) 83–102.